

A multi-chroic kinetic inductance detectors array using hierarchical phased array antenna

Shibo Shu^{1,†} · Andrew Beyer² · Peter Day² ·
Fabien Defrance¹ · Jack Sayers¹ · Sunil Golwala¹

the date of receipt and acceptance should be inserted later

Abstract We present a multi-chroic kinetic inductance detector (KID) pixel design integrated with a broadband hierarchical phased-array antenna. Each low-frequency pixel consists of four high-frequency pixels. Four passbands are designed from 125 to 365 GHz according to the atmospheric windows. The lumped element KIDs are designed with 100 nm Al as the inductor and with Nb parallel plate capacitors using hydrogenated amorphous Si as the dielectric. Due to the broadband coverage, two different types of structures are needed to couple light from microstrip lines to the KIDs. The KIDs designs are optimized for a 10-m-class telescope at a high, dry site.

Keywords kinetic inductance detector, photon noise limited, NbTiN

1 Introduction

Multi-chroic kinetic inductance detectors (KIDs) are essential technology for future ground-based telescopes [1, 2]. In the millimeter and sub-millimeter range, the optimal pixel size and spacing vary with frequency. For a multi-chroic pixel, the fixed pixel spacing would not allow all bands to achieve the optimal mapping speed, especially when more than two bands exist. One way to solve this problem is using a hierarchical focal plane array [3]. Here we present a hierarchical pixel design using a slot-antenna array with KIDs being used as detectors. The long-term goal of this work is to make a hierarchical focal plane array covering 75-415 GHz with 6 bands, detailed in Table 1, for future ground-based large telescopes. As a technology demonstration, here we present a 2-scale design with 4 frequency bands from 125 to 365 GHz (Band 2-4).

2 Hierarchical focal plane design

Slot antenna array has been successfully used by the BICEP collaboration [5] and in the MUSIC instrument [6]. Compared to usual resonant slot antenna [7], we made a non-resonant

¹ California Institute of Technology, Pasadena, California 91125, USA

² Jet Propulsion Laboratory, California Institute of Technology, Pasadena, California 91109, USA

[†]E-mail: shiboshu@caltech.edu

Band	1	2	3	4	5	6
λ [mm]	3.3	2	1.33	1.05	0.85	0.75
ν [GHz]	90	150	230	290	350	400
$\Delta\nu$ [GHz]	35	47	45	40	34	30
P_{opt} [pW]	4.0	8.6	8.5	9.9	12	17
l_{antenna} [mm]	6.66	6.66	3.33	3.33	1.66	1.66
Optimized results						
f_r [MHz]	125	175	225	275	325	375
A_{Ctot} [mm ²]	7.2	3.7	2.2	1.5	1.0	0.8
Q_r [$\times 10^4$]	1.7	1.0	1.0	0.8	0.7	0.5
n_{qp} [μm^{-3}]	2619	3422	2889	3022	3216	3901
τ_{qp} [μs]	37	28	33	32	30	25
NEP _{photon} [aW/ $\sqrt{\text{Hz}}$]	34	64	70	85	109	157
NEP _{gr} [aW/ $\sqrt{\text{Hz}}$]	21	34	40	45	51	62
NEP _{amp} [aW/ $\sqrt{\text{Hz}}$]	4	11	13	17	24	38
NEP _{TLS} [aW/ $\sqrt{\text{Hz}}$]	4	9	12	17	23	34
NEP _{tot} [aW/ $\sqrt{\text{Hz}}$]	41	74	83	99	125	176

Table 1 Specifications of optical bands [4] and typical design parameters after optimization.

slot antenna design, which has a broadband efficiency and allows 6 bands placed inside, shown in Fig. 1. As the slot is long, only one polarization is allowed. For this 2-scale design, the smallest pixel has a slot length of 3.33 mm for Band 3-5, and four small pixels added together to be a large pixel for Band 2.

2.1 Millimeter-wave coupler

To couple millimeter-wave signal to KIDs, we designed two couplers with capacitively coupling between the millimeter-wave microstrip transmission line and the KID inductor. For low frequency bands (Band 1-3), the wavelength is >1 mm long, so the Al inductor is designed to follow the signal traveling direction and serves as a lossy microstrip. For high frequency bands (Band 4-6), the wavelength is much shorter and the signal can be fully attenuated at the half way of the inductor in the low frequency coupler design, so we let the inductor be perpendicular to the signal direction and the attenuation of signal is determined by how much signal goes in to each perpendicular Al line. To let the signal go through the perpendicular Al line, a 180-degree phase shifter is used to alter the sign of the electromagnetic field making a voltage difference between two coupling pads. The coupling is tuned by the area of the coupling fingers on the two sides of the inductor. With proper setup, a near-uniform absorption is achieved in the inductor. This high frequency coupler design is detailed in Ref. [4, 8].

2.2 Optimization of the KID design

The thickness of Al is designed to be 100 nm with a transition temperature of 1.3 K, a sheet resistance of $0.069 \Omega/\square$, and a sheet inductance of $0.11 \text{ pH}/\square$. The Al lumped-element inductor has a magnetic inductance of $6.85 \text{ nH}/\text{mm}$ and the kinetic inductance ratio is 26% with an inductor width of $1 \mu\text{m}$. Nb parallel plate capacitors with 800-nm thick aSi are used for tuning the resonance frequency. To find the optimal KID design, we selected the horizontal inductor size l_{abs} (Fig. 2), and the resonance frequency f_r as sweeping parameters. The

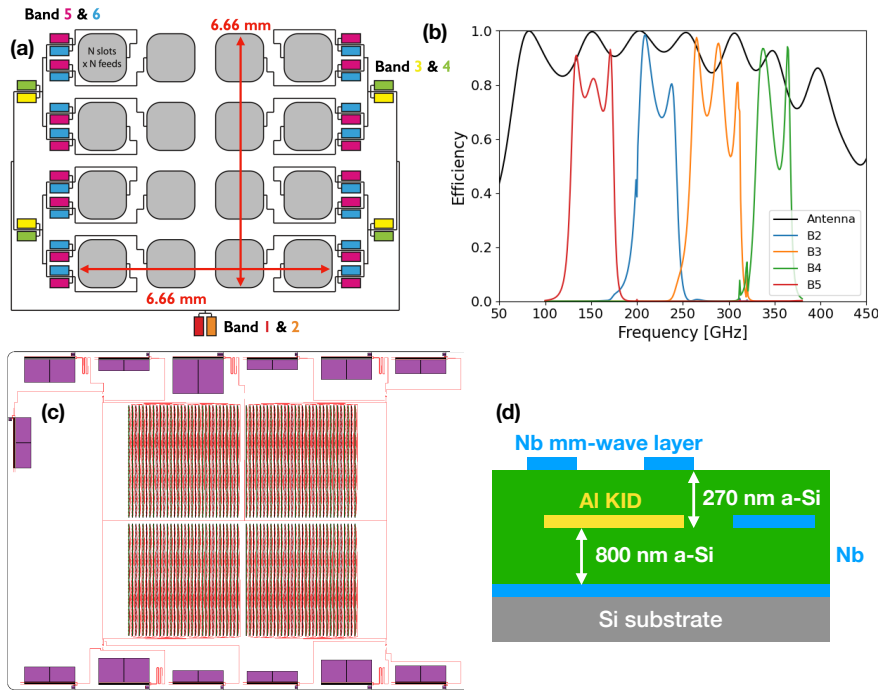


Fig. 1 (a) The concept of an ultimate hierarchical pixel design with 6 bands. (b) Antenna efficiency assuming a perfect anti-reflection layer. The four bandpass filter efficiencies in design are also plotted. (c) The mask of a 2-scale pixel design, which has 13 KIDs. (d) The material stack-up.

coupling quality factor is set to be the same with the internal quality factor Q_i . The capacitor area is calculated from f_r . We first calculate the noise equivalent power (NEP) and use the mapping speed $1/(\text{NEP}^2 \times \text{Area})$, which takes the pixel area into account, to find the optimal design. $Q_r > 10^4$ is set to have a reasonable multiplexing factor. Taking the optimization results of 6 bands, we decide to have $l_{\text{abs}} = 1.5$ mm. Resonance frequencies from B1 to B6 are designed to be from 100 MHz to 400 MHz with 50 MHz span for each band. Some typical optimization results are shown in Table. 1.

3 Dark and blackbody measurement

After fabrication, we performed one dark run and one blackbody run. 50 KIDs are measured out of 56 in design. By fitting the temperature sweep shown in Fig. 4, $T_c = 1.29$ K and $\alpha = 0.26$ are extracted, consistent with the design ones. Quasiparticle lifetime of 100 μs , shorter than expected, is fitted from cosmic-ray events at 250 mK. Combining the noise and the responsivity, we calculated the dark NEP of $2.2 \times 10^{-17} \text{ W}/\sqrt{\text{Hz}}$, lower than the photon NEP in design (Fig. 4).

In blackbody measurement, the array was at 290 mK with blackbody temperature sweeping from 4 K to 6 K. Using the responsivity and the resonance frequency shift, the optical efficiency is calculated for each resonator, shown in Fig. 4. As the anti-reflection coating [9] is optimized for 170-300 GHz (-10 dB), the Band 3 resonators show a higher efficiency and

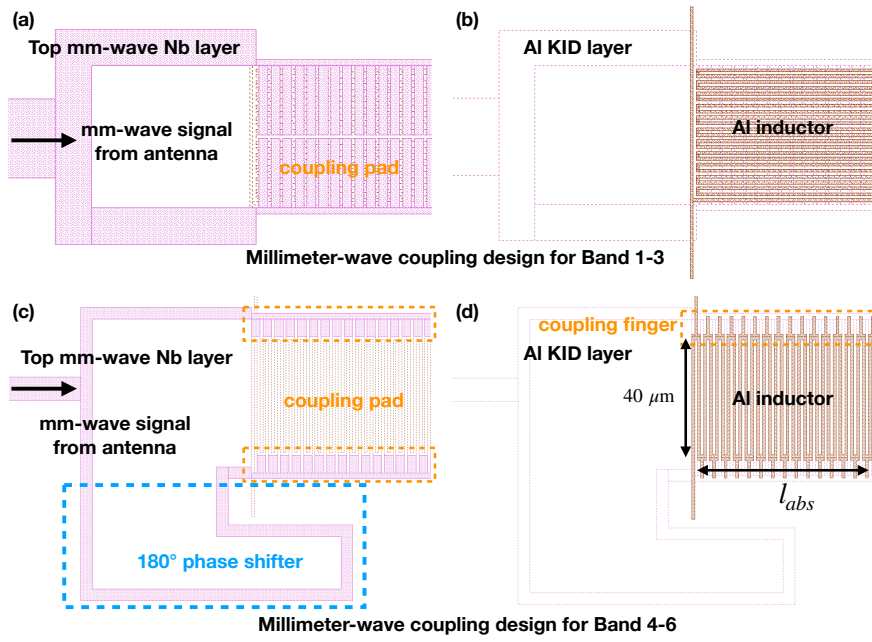


Fig. 2 Two millimeter-wave coupler designs. (a) and (b) are the design for B1-3 and (c) and (d) are the design for B4-6.

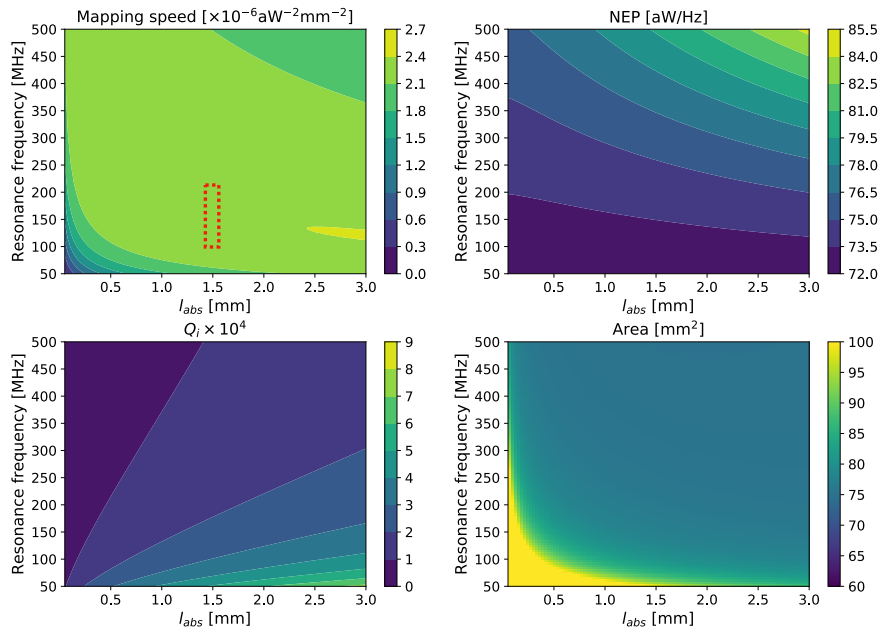


Fig. 3 Four parameters calculated in optimization of Band 2. The dashed red line shows where the final design is made.

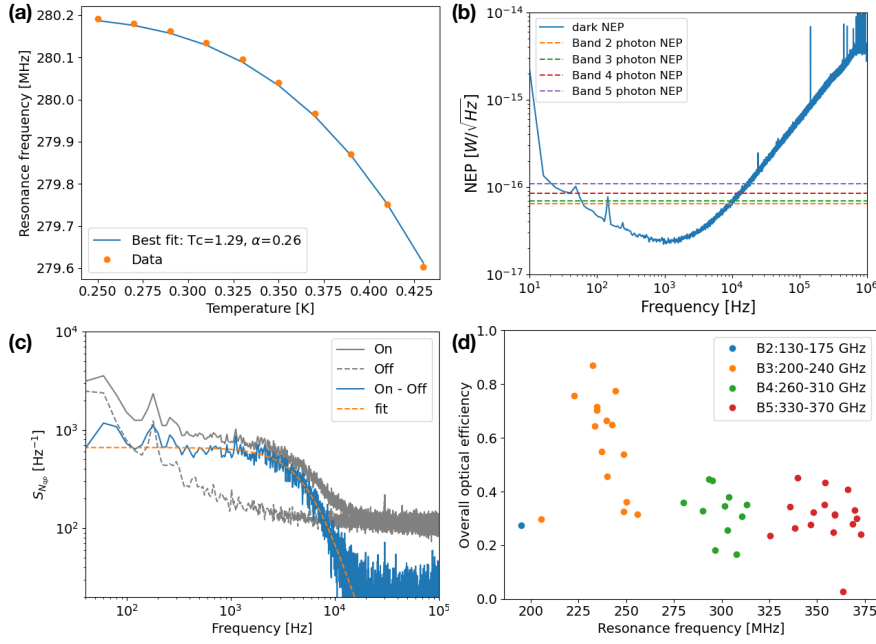


Fig. 4 (a) Temperature sweep of resonance frequency. (b) Dark NEP in phase direction. (c) Quasiparticle generation-recombination noise at 290 mK in phase direction. (d) Optical efficiency (with pair breaking efficiency excluded) calculated from blackbody temperature sweep.

the other bands show a lower efficiency. In the next step, we will use Fourier transform spectrometer to detail the spectral characterization.

The quasiparticle generation-recombination noise was measured from a dark resonator in phase direction, shown in Fig. 4. From fitting, the quasiparticle lifetime of $25 \mu s$ and quasiparticle density of $2001 / \mu m^3$ are extracted, consistent with $25 \mu s$ and $2026 / \mu m^3$ calculated from the simplified Mattis-Bardeen theory [10].

4 Conclusion

We have shown a new multi-choic kinetic inductance detectors array design using broadband hierarchical phased-array antenna. The dark and blackbody measurements suggest the array performance is as expected. Further measurements are needed for beam characterization.

The datasets generated during and analysed during the current study are available from the corresponding author on reasonable request.

References

1. P. K. Day, H. G. LeDuc, B. A. Mazin, A. Vayonakis, and J. Zmuidzinas. *Nature* **425**, 6960, 817 (2003).
2. L. Perotto, N. Ponthieu, J. Macías-Pérez, R. Adam, P. Ade, P. André, A. Andrianasolo, H. Aussel, A. Beelen, A. Benoît, et al. *Astronomy & Astrophysics* **637**, A71 (2020).

3. A. Cukierman, A. T. Lee, C. Raum, A. Suzuki, and B. Westbrook. *Applied Physics Letters* **112**, 13, 132601 (2018).
4. C. Ji. *Design of Antenna-Coupled Lumped-Element Titanium Nitride KIDs for Long-Wavelength Multi-Band Continuum Imaging*. Ph.D. thesis, California Institute of Technology (2015).
5. P. A. Ade, R. Aikin, M. Amiri, D. Barkats, S. Benton, C. A. Bischoff, J. Bock, J. Brevik, I. Buder, E. Bullock, et al. *The Astrophysical Journal* **792**, 1, 62 (2014).
6. S. R. Golwala, C. Bockstiegel, S. Brugger, N. G. Czakon, P. K. Day, T. P. Downes, R. Duan, J. Gao, A. K. Gill, J. Glenn, M. I. Hollister, H. G. Leduc, P. R. Maloney, B. A. Mazin, S. G. McHugh, D. Miller, O. Noroozian, H. T. Nguyen, J. Sayers, J. A. Schlaerth, S. Siegel, A. K. Vayonakis, P. R. Wilson, and J. Zmuidzinas. In W. S. Holland, editor, *SPIE Astronomical Telescopes + Instrumentation*, page 845205. SPIE (2012).
7. A. Goldin, J. J Bock, J. J Bock, A. E Lange, A. E Lange, H. LeDuc, A. Vayonakis, and J. Zmuidzinas. *Nuclear Instruments and Methods in Physics Research Section A: Accelerators, Spectrometers, Detectors and Associated Equipment* **520**, 1-3, 390–392 (2004).
8. C. Ji, A. Beyer, S. Golwala, and J. Sayers. In *Millimeter, Submillimeter, and Far-Infrared Detectors and Instrumentation for Astronomy VII*, volume 9153, page 915321. International Society for Optics and Photonics (2014).
9. F. Defrance, C. Jung-Kubiak, J. Sayers, J. Connors, C. deYoung, M. I. Hollister, H. Yoshida, G. Chattopadhyay, S. R. Golwala, and S. J. Radford. *Applied optics* **57**, 18, 5196–5209 (2018).
10. J. Zmuidzinas. *Annual Review of Condensed Matter Physics* **3**, 1, 169–214 (2012).